Photoresponsive Polymers

DOI: 10.1002/ange.201106777

Photocontrol of the Translocation of Molecules, Peptides, and Quantum Dots through Cell and Lipid Membranes Doped with Azobenzene Copolymers**

*Sarra C. Sebai, Dimitra Milioni, Astrid Walrant, Isabel D. Alves, Sandrine Sagan, Cécile Huin, Loic Auvray, Dominique Massotte, Sophie Cribier, and Christophe Tribet**

Permeabilization of lipid membranes is a major challenge for the development of biocides and for improving the delivery of DNA, anticancer agents, and small proteins within the cell cytosol. Effective membrane permeabilization can be achieved by chemical techniques that often involve an intramembrane assembly of permeabilizing agents such as peptides,[1–3] amphiphilic molecules, or polymers.[4,5] Alternative physical techniques are electroporation or microinjection. A present challenge for chemical approaches lies in targeting cells while maintaining cell viability.[6,7] The development of permeabilizers for the remote control of membrane properties is accordingly in high demand to compete with microinjection, because the former avoids mechanical damage and addresses large cell subsets.

The strategy consists of using so-called "smart" systems, that is, tailoring stimuli-responsive molecules to affect lipid membranes.[4,8–12] The variation of the pH value has been the major focus for the design of smart bilayers doped with polymers[11,12] or peptides[13] with the goal of delivering substances of interest in the late endosomes or targeting acidic tumors.[14] However, light-responsive systems would offer a more versatile and external trigger. To photocontrol self-assembly and/or interaction with lipid bilayers several authors had recourse to amphiphilic azobenzene derivatives.[15,16] The best achievements in this field show a modulation of the rate of transmembrane release of small molecules from liposomes, the membranes of which contain either a pore-forming peptide, gramicidin, conjugated to azobenzene[17] or an azobenzene-containing lipid.[18] However, except for highly specific photogating by engineered membrane proteins,[19] no artificial system (likely less specific than protein gates) enabled phototriggered permeabilization on living cells. So far, in regard to large molecules (e.g. peptides), their pH-controlled passage was essentially achieved using polymer carriers. Herein, we show that azobenzene-modified polymers (AMPs; Scheme 1)[20] can impart plasma membranes of living cells and vesicles with this desirable photoresponse.

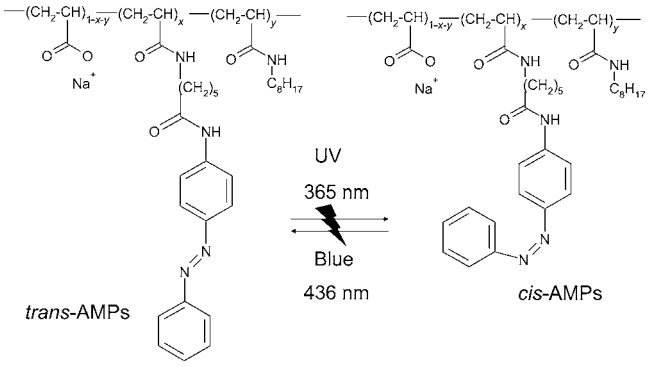

Scheme 1. Structure of AMPs and *cis–trans* photoisomerization. Typically $x = 10$ and $y = 15$ mol% (see text and the Supporting Information).

The photocontrolled delivery of a small peptide was tested in CHO mammalian cells. A well-characterized basic peptide, RL9 (RRLLRRLRR-NH_2; R = Arg = arginine, L = Leu = leucine), that binds to cell surfaces without crossing membranes[22] was added to cells and incubated in the presence of AMP, which is predominantly in its *cis* form. *cis*-AMP was prepared as described in the Supporting Information by pre-exposure to UV light (365 nm) so that cells were not exposed to UV light. *trans*-AMP was generated in situ by exposing half of the wells containing cells to blue light (436 nm) for two minutes. Images of cells in Figure 1a were obtained by using a biotinylated RL9 derivative; the cells were incubated for one hour with either *cis*- or *trans*-AMP and labeled with streptavidine-AlexaFluor488 (see the Experimental Section). The diffuse green fluorescence in samples exposed to blue light (*trans*-AMP) shows a homogeneous internalization that differs from punctuated images

[*] Dr. S. C. Sebai, Dr. C. Tribet
Ecole Normale Supérieure, Departement de Chimie, UMR 8640 CNRS-ENS-UPMC
24, rue Lhomond, 75005 Paris (France)
E-mail: christophe.tribet@ens.fr
D. Milioni, Dr. A. Walrant, Dr. I. D. Alves, Dr. S. Sagan, Prof. S. Cribier
UPMC Univ Paris 06, UMR 7203 CNRS-UPMC-ENS
4, Place Jussieu, 75005 Paris (France)
Dr. C. Huin, Dr. L. Auvray
LAMBE UMR8587, UEVE-CNRS-CEA
Bd F. Mitterrand, 91025 Evry (France)
D. Massotte
IGBMC
1 rue Laurent Fries, 67400 Illkirch (France)

[**] This work was supported by the ANR for the award of Grant photochannels N° ANR-07-BLAN-0278. The authors thank Déborah Cardoso for providing Figure S4 and F. Pinaud and M. Dahan for providing Qdots.

Supporting information for this article is available on the WWW under http://dx.doi.org/10.1002/anie.201106777.

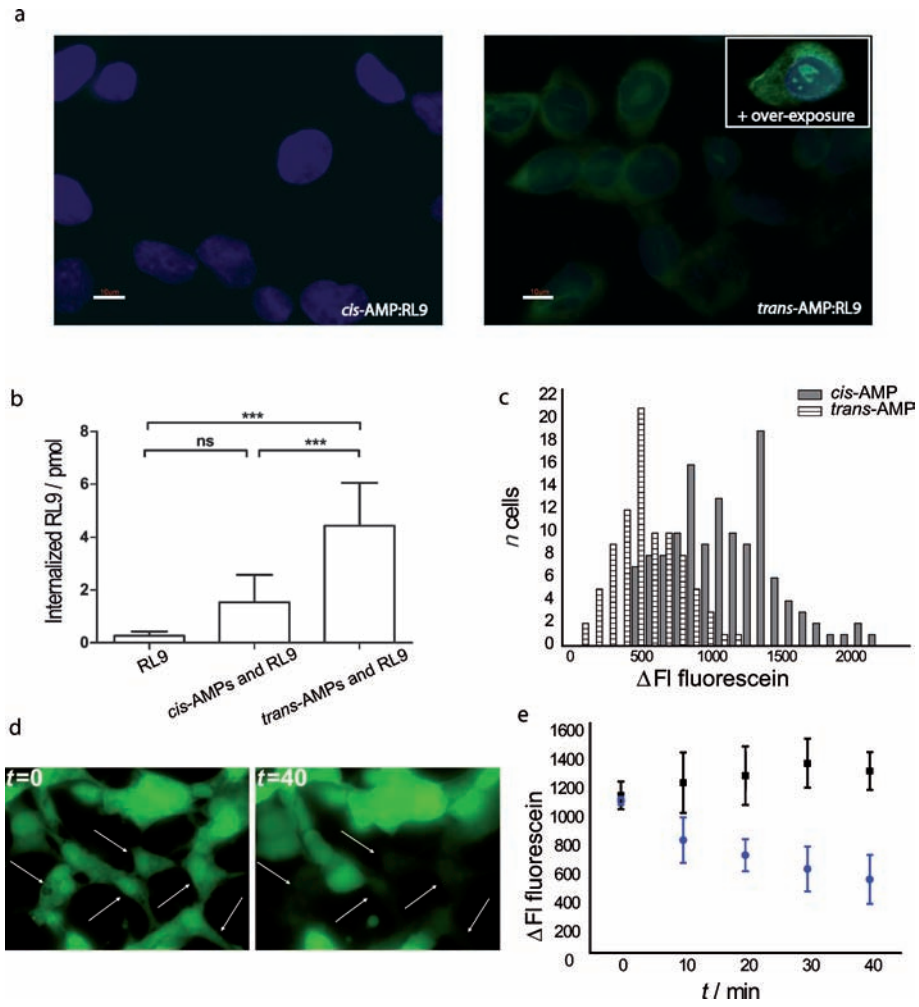

Figure 1. Effect of a *cis*- or *trans*-AMP ($x = 0.10$, $y = 0.15$ in Scheme 1) on cell permeabilization. *cis*-AMP was added to cells at 2 $\mu g\,mL^{-1}$ and switched to the *trans* form in half of the wells by exposure to blue light. a) Fluorescence images of CHO cells incubated for one hour with biotinylated RL9 and *cis*- or *trans*-AMP as quoted. Cells were labeled with both streptavidine-AlexaFluor488 (green) and 4′,6-diamidino-2-phenylindole (DAPI; blue) after fixation. Scale bars correspond to 10 μm. Over-exposed image on the upper right panel shows more clearly the RL9 distribution in the cell upon incubation with *trans*-AMP. b) Quantification of internalized RL9 peptide in CHO cells in the presence of *cis*-AMP or *trans*-AMP (see text for details). Significance was tested using one-way analysis of variance (ANOVA) and subsequent Tukey's multiple comparison test, ns: $p > 0.05$, *** : $p < 0.001$. c) Histogram of CFDA intracytosolic fluorescence intensity over a group of 100 COS cells after 40 min and incubation with *cis*- or *trans*-AMP. d) CFDA-labeled COS cells shown after addition of AMP at $t = 0$ min. Cells permeabilized at $t = 40$ min are indicated by arrows. e) Release kinetics of CFDA measured by detecting the intracytosolic fluorescence ΔFI (averaged on three independent groups of 10 cells each) during incubation with *cis*-AMP (black squares) or *trans*-AMP (blue dots).

commonly obtained after endocytosis. The fluorescence of cells incubated with *cis*-AMP was significantly lower and is not distinguished from the fluorescence achieved with the parent chain poly(acrylic acid) (PAA), which is devoid of hydrophobic side groups (see controls in the Supporting Information). This observation suggests a markedly lower internalization with *cis*-AMP (or PAA) compared to that achieved with *trans*-AMP. Quantification of internalized RL9 was performed by MALDI-TOF mass spectrometry[23] (see the Experimental Section for protocols). We can see from Figure 1 b that RL9 internalization is dependent on the AMP isomerization state. *cis*-AMP does not significantly improve RL9 internalization, compared to control experiments in the absence of AMPs ((1.5 ± 1) vs. (0.3 ± 0.2) pmol of peptide in one million cells, respectively), whereas RL9 is significantly internalized in cells treated with *trans*-AMP. About 4.5 pmoles of RL9 (corresponding to an intracellular concentration of approximately 4 μM under the assumption of an intracellular volume of 1 pL) are delivered to the cytosol of cells, an amount similar to the cell-penetrating peptide penetratin.[24] In the absence of AMPs, the amount of internalized RL9 remained negligible as reported.[22] We can therefore postulate that *trans*-AMP delivers small peptides to cells in a light-responsive manner. These conditions ensured the absence of toxicity. Toxicity of AMP is not detected up to a polymer concentration of 1 $mg\,mL^{-1}$, that is, three orders of magnitude above the present conditions of photopermeabilization (for toxicity assays see the Supporting Information).

Light-driven permeabilization could be nonspecific and share similarities with polymer-triggered pore formation described with hydrophobically modified poly(acrylic acid) devoid of photoresponsive groups.[9,25] This hypothesis would imply that the permeabilization controlled by AMPs should not markedly depend on a specific protein machinery and should in addition induce photorelease of cytosolic molecules as well as delivery. To confirm this hypothesis, we investigated first the leakage of cell-encapsulated probes. Second, membrane permeabilization in the absence of proteins was illustrated by experiments on artificial lipid membranes.

Phototriggered release from living cells was demonstrated by using a cell-encapsulated fluorescein probe. Figure 1 d shows viable mammalian COS cells that were grown on glass coverslips and fluorescently labeled with 6-carboxyfluorescein diacetate (CFDA), a molecule that infuses through the membrane in its ester form and is trapped in cells in its anionic form after hydrolysis by cytosolic esterases (see the Experimental Section). *cis*-AMP was added at time zero after washing out the excess CFDA. No CFDA leakage is observed

in cells exposed to predominantly *cis*-AMP (Figure 1e). In contrast, the leakage curve shown in Figure 1e shows that a gradual drop of the average intracellular fluorescence is triggered by exposure to blue light at time zero, that is, immediately upon formation of *trans*-AMP. The AMPs polarity hence controls the level of fluorescence within the cells. For this kinetics study, however, the reference experiment with *cis*-AMP (no leakage) needed short (1 s) exposures to UV light to preserve predominantly the *cis* state while taking pictures (requiring blue light) of fluorescein distribution (one picture every 10 min). Exposure of cells to UV light is not needed in practice to achieve the photocontrol of leakage: in another set of experiments, fluorescently labeled COS cells were supplemented with preformed *cis*-AMP. Cells were then incubated in the dark for 40 min. In the dark the predominant *cis* form of AMP can be preserved for hours. *trans*-AMP was formed in situ by exposure to blue light at time zero. Figure 1c presents the distribution of the fluorescence intensity of CFDA in cells treated with either *cis*- or *trans*-AMP (population of $N \approx 100$ cells). Cells incubated with *cis*-AMP are characterized by a more intense average fluorescence (FI; $\Delta FI \approx 1100$) compared to cells treated with *trans*-AMP ($\Delta FI \approx 500$). Impermeable and fully loaded cells in the absence of AMPs (as a control) exhibited fluorescence around the average $\Delta FI \approx 1400$. As reflected by the broad fluorescence distribution, heterogeneities exist in the cell population. The significant shift of the mean fluorescence intensity noticeable between cells treated with *cis*-AMP and *trans*-AMP confirms, however, that *trans*-AMP allows a more rapid release of a small anionic soluble dye through the plasma membrane. We then wondered if molecules with larger radii, such as small endogenous soluble proteins, are released. We expressed soluble enhanced green fluorescent protein (eGFP) in COS cells and monitored the fluorescence of the protein in the cell after treatment with AMP. No effects of either *trans*- or *cis*-AMP were detected over an hour, thus suggesting that we are dealing with a size limitation in the permeabilization efficiency (see the Supporting Information). The retention of intracytosolic proteins is of major importance and is consistent with the absence of toxicity of AMP (see the Supporting Information) and preservation of cell viability upon incubation with *trans*-AMP that we previously showed under similar conditions.[21]

Electrophysiology experiments were then conducted on artificial planar lipid membranes (also called black lipid membranes, BLM). This method enables direct monitoring of membrane permeability by probing current traces across the bilayer. A typical signature for an impermeable membrane is identified by a stable current trace with no associated conductance at a fixed applied voltage of −100 mV across the membrane (signal similar to that shown in Figure 2d in the presence of *cis*-AMP). In contrast, the presence of the same concentration (1 μg mL^{-1}) of *trans*-AMP generates variable currents (Figure 2a,b). These signals are characteristic of passage of ions, and abrupt jumps of current from zero to plateau values suggest the fast opening of pores in the bilayer.[26] Typically, the current varies slightly during the first 15 min after membrane formation (e.g. Figure 2a, part 1). Hence, the membrane likely remains mainly closed at the

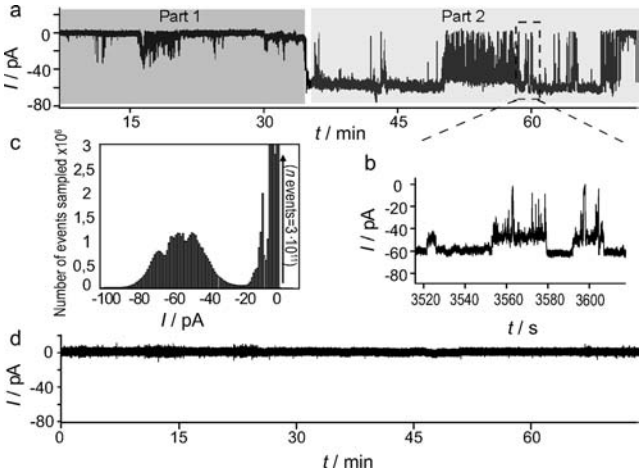

Figure 2. Current-trace measurements through a black lipid membrane monitored after supplementation with AMP in the anodic compartment (pH 7.0). The voltage applied is −100 mV (for detailed experimental conditions see the Supporting Information). a) Incubation with *trans*-AMP. b) Magnification of a region of fluctuations between permeant states. c) Histograms of current occurrence during measurement over approximately one hour for five runs (five different membranes). d) Current trace in the presence of *cis*-AMP at pH 7 showing no permeabilization.

onset of the interaction with *trans*-AMP (see the Supporting Information for current histograms). However, after about 30 min incubation (Figure 2a, part 2) discrete current jumps persist till the end of the run, indicating long-lasting permeant structures. Figure 2c shows the histogram of the times lapsed by the membrane in its "open" states. A broad distribution of currents is revealed, with one peak corresponding to "closed" (0 pA), a second centered at −8 pA, and a third broader peak at about −60 pA. This broad distribution reflects a multiplicity, and/or fluctuation, of structures of *trans*-AMP-formed pores, which we have not investigated yet. The dispersity of opening events suggests that AMPs in their more hydrophobic *trans* form induce dynamic pore formation. Penetration of hydrophobic polymers in the hydrophobic core of a bilayer can scramble lipid organization.[10] In contrast, preservation of the impermeable state when AMPs were added in their more polar *cis* form suggests a penetration to a lesser extent of *cis*-AMP in the membrane (note that *cis*-AMP was shown however to tightly bind to membranes, as shown for the preparation of giant unilamellar vesicles (GUV); see the Supporting Information).

The structure of polymers significantly affects their interaction with the membrane, and for instance longer polymer chains destabilize lipid bilayers at higher pH values.[8] We compared AMPs having the same backbone but a slightly different degree of modification with octyl and azobenzene side groups to vary the hydrophobicity of the chains ($x = 10$ or 5 mol% in Scheme 1). Giant vesicles with AMPs inserted in their membrane were prepared by electroformation (see the Supporting Information) in buffer containing the water-soluble fluorescein-labeled probe, dextran-FITC. The diameters of the spherical giant vesicles, called pol-GUVs, ranged from 10 to 80 μm (Figure 3a). Pol-GUVs were

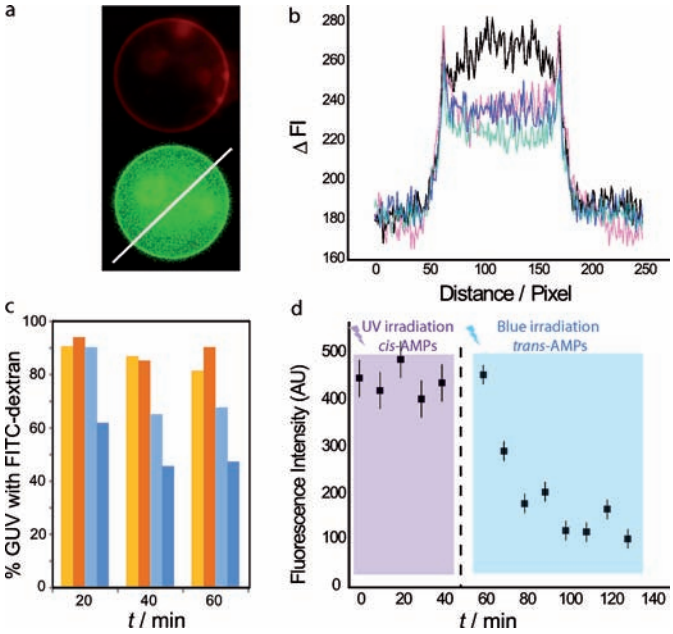

Figure 3. Leakage of dioleoylphosphatidylcholine (DOPC) pol-GUVs revealed by epifluorescence. a) Images of one pol-GUV of approximately 37 μm in diameter with encapsulated QDs (green) at pH 7 and DPPE-rhodamine (DPPE = dipalmitoylphosphatidylethanolamine sulforhodamine; red). b) Fluorescence profile along diameter (white line in (a)) showing the decrease of internal fluorescence from a GUV containing trans-AMPs (0.1 g/g AMPs/DOPC ratio) at 0 min (black line), 10 min (red line), 20 min (blue line), and 40 min (green line) after irradiation with blue light. Scale: 10 pixels = 2.2 μm. c) Fractions of dextran-containing pol-GUV in a random sampling of approximately 150 GUVs. Two polymers were used with fractions of azobenzene (x in Scheme 1) of 0.1 ("10azo") or 0.05 ("5azo"). AMP/DOPC ratios are 0.01 g/g for the yellow (5azo) and light blue (10azo) bars and 0.05 g/g for the red (5azo) and dark blue (10azo) bars. GUVs were diluted under UV light and exposed to blue light at time zero (see text for definition of empty GUVs). d) Delayed release of QDs from an isolated pol-GUV in cis-AMP form (t = 0 min to t = 40 min, then switched under blue light to the trans-AMP form (t = 60 min to t = 130 min). Error bars indicate standard deviations calculated from the spatial noise of the fluorescence in both the background and in the GUV.

diluted in the microscope observation chamber under exposure to UV light to reach the predominantly *cis*-AMP state. The fluorescence profile across the vesicle diameter is indicative of the amount of GUV-encapsulated dextran. For simplicity, we distinguished between "empty" and "loaded" GUVs on the basis of the absence or presence of internal fluorescence (the fluorescence intensity threshold for empty GUVs was fixed arbitrarily at the background fluorescence plus twice the noise). In a first set of experiments, pol-GUVs prepared at an AMP/lipid ratio of 0.05 or 0.01 g/g were exposed to blue light (two minutes) just after dilution at pH 7.0. In Figure 3c, the fraction of "dextran-containing" pol-GUV is plotted against increasing incubation times after switching on the light. In the absence of AMP or in the presence of AMP having lower hydrophobicity (here 15 mol% octyl and 5 mol% azobenzene), dextran is essentially kept entrapped in GUV for one hour. In contrast, a significant leakage of dextran is observed after exposure of pol-GUV containing AMPs with 15% octyl and 10% azobenzene (i.e. the polymer also used in experiments on cells) to blue light. This feature confirms the ability of AMPs to help translocation of large molecules. Membrane integrity was preserved while permeabilization occured, which was already observed for other hydrophobically modified polymers.[9,25]

Moreover, we confirmed the possibility for nanometer particles to cross the membrane by performing leakage experiments on isolated GUVs loaded with soluble quantum dots (QDs) as fluorophores (see the Supporting Information, radius 4.2 nm)[27] and AMP (10 mol% azobenzene) in the membrane. QDs were not bleached during the experiment, which enabled us to record leakage kinetics. Fluorescence intensity across a diameter indicates the presence of soluble QDs as described in reference [28]. Release of QDs upon exposure of pol-GUVs to blue light is shown in Figure 3b,d. In contrast, no leakage was observed during one hour when UV light was constantly shone on pol-GUV (leakage can then be triggered after 60 min; Figure 3d shows a representative example). Hence, we show that AMPs with a high enough density of azobenzene in the chain allow controlled release of macromolecules and nanoparticles such as dextran and QDs.

On the mechanistic side, polymer binding to lipid bilayers is known to affect the local assemblies of lipids and induces, for instance, lateral lipid segregation or membrane thinning.[4,9] The interaction between amphiphilic copolymers and liposomes is modulated by their apparent hydrophobicity,[25] which in AMPs is controlled by light:[21] destabilization of the membrane occurs upon *cis* to *trans* isomerization of the AMPs, likely owing to deeper penetration of *trans*-azobenzene hydrophobic groups in the bilayer.[29] AMPs are promising nonspecific tools for controlling the permeability of plasma membranes in physiological conditions (such as in culture medium) and more importantly phototriggered internalization of peptides in living cells. Furthermore, they bring on a control of the opening of artificial pores and passage of macromolecules through lipid bilayers; these latter points will help to study the dynamics of biomimetic gates and delivery systems.

Experimental Section

The Supporting Information describes polymer synthesis, toxicity assays, *cis–trans* isomerization, controls, GFP transfection, and details on current measurements.

RL9 (RRLLRRLRR-NH_2) cellular uptake: Chinese Hamster Ovary CHO-K1 cells were cultured in Dulbecco's modified Eagle's medium (DMEM) supplemented with 10% foetal calf serum (FCS), penicillin (100000 IU/L), streptomycin (100000 IU/L), and amphotericin B (1 mg L^{-1}) in a humidified atmosphere containing 5% CO_2 at 37 °C. AMP (2 or 16 μg mL^{-1}) was added to preseeded CHO cells (10^6) in the presence of RL9 (10 μM) or added to cells 30 min prior to RL9 addition. The order of addition made no difference to the results. Experiments were carried out in triplicate, on different cell batches. RL9 was incubated for one hour at 37 °C in both conditions. RL9 cellular uptake was quantified by using the method described by Burlina et al.[23] except that membrane-bound RL9 was efficiently removed by sequential washing steps made of Hank's buffered salt solution (HBSS), 1M NaCl/HBSS, trypsin, 1M NaCl/HBSS, HBSS, so that only internalized RL9 would be quantified. Final trypsinization

(5 min at 37 °C) resulted in removal of external peptide and the detachment of cells, which were then collected and lysed in Triton X100 (0.3 %) and NaCl (1 M) at 100 °C. Lysates were incubated with streptavidin-coated magnetic beads to extract RL9, which was later eluted with α-cyano-4-hydroxycinnamic acid (HCCA) matrix and spotted on the MALDI plate. Deuterated RL9 (1.5 pmol) was used as an internal standard, and RL9 in cell lysates was quantified by MALDI-MS.[22,24] Fluorescence images of the distribution of RL9 biotinylated at the N terminus were recorded after incubation in the same conditions as for RL9 prior to the fixation of cells (4 % paraformaldehyde pH 7.4 for 15 min at room temperature), TX100 permeabilization (0.3 % for 5 min), and labeling by streptavidine-AlexaFluor488. Nuclei were stained with DAPI. All images were recorded under the same excitation conditions by using the same exposure time and objective (x100 PlanFluor, inverted NikonEclipse microscope).

Carboxyfluorescein diacetate cell encapsulation and release: COS cells were grown in DMEM supplemented with 10 % FCS and glutamine (2 mM) at 37 °C and 5 % CO_2. COS cells were preseeded (50 000 cells) on MatTek (MatTek Corporation Ashland, MA, USA) glass bottom dishes (35 mm) in complete medium the day before the experiment. 6-carboxyfluorescein diacetate (Sigma Aldrich) was added at 100 μM in serum-free DMEM for 30 min at 37 °C in a CO_2 chamber. Esterases present in the cytoplasm hydrolyze it into encapsulated carboxyfluorescein. Excess CFDA was removed by washing the cells in serum-free DMEM. AMP (2 $\mu g\,mL^{-1}$) was irradiated with UV light for 15 min in serum-free DMEM (1 mL) and then added to COS cells. For "*cis* conditions", cells were maintained in the dark. For "*trans* conditions", cells were irradiated for 30 seconds either at 436 nm (or 476 nm through the microscope objective). Fluorescence images were recorded by using a LEICA DM-IRE2 inverted microscope under fixed exposure conditions (typical exposure time 500 ms, binning 2 × 2). To determine fluorescence intensities, the average background intensity was subtracted from the intensity measured inside the vesicle or the cell for every single frame.

Received: September 23, 2011
Revised: November 9, 2011
Published online: January 19, 2012

Keywords: azobenzenes · membranes · photochromism · polymers · vesicles

[1] S. M. Butterfield, H. A. Lashuel, *Angew. Chem.* **2010**, *122*, 5760 – 5788; *Angew. Chem. Int. Ed.* **2010**, *49*, 5628 – 5654.
[2] S. B. Fonseca, M. P. Pereira, S. O. Kelley, *Adv. Drug Delivery Rev.* **2009**, *61*, 953 – 964.
[3] G. Bocchinfuso, A. Palleschi, B. Orioni, G. Grande, F. Formaggio, C. Toniolo, Y. Park, K. S. Hahm, L. Stella, *J. Pept. Sci.* **2009**, *15*, 550 – 558.
[4] W. H. Binder, *Angew. Chem.* **2008**, *120*, 3136 – 3139; *Angew. Chem. Int. Ed.* **2008**, *47*, 3092 – 3095.
[5] H. Cheradame, M. Sassatelli, C. Pomel, A. Sanh, J. Gau, L. Bacri, L. Auvray, P. Guégan, *Macromol. Symp.* **2008**, *261*, 167 – 181.
[6] T. M. Allen, P. R. Cullis, *Science* **2004**, *303*, 1818 – 1822.
[7] V. P. Torchilin, A. N. Lukyanov, *Drug Discovery Today* **2003**, *8*, 259 – 266.
[8] J. L. Thomas, D. A. Tirrell, *Acc. Chem. Res.* **1992**, *25*, 336 – 342.
[9] C. Tribet, F. Vial, *Soft Matter* **2008**, *4*, 68 – 81.
[10] H. Ringsdorf, J. Venzmer, F. M. Winnik, *Angew. Chem.* **1991**, *103*, 323 – 325; *Angew. Chem. Int. Ed. Engl.* **1991**, *30*, 315 – 318.
[11] T. Chen, D. McIntosh, Y. H. He, J. Kim, D. A. Tirrell, P. Scherrer, D. B. Fenske, A. P. Sandhu, P. R. Cullis, *Mol. Membr. Biol.* **2004**, *21*, 385 – 393.
[12] M. A. Yessine, J. C. Leroux, *Adv. Drug Delivery Rev.* **2004**, *56*, 999 – 1021.
[13] Y. K. Reshetnyak, O. A. Andreev, M. Segala, V. S. Markin, D. M. Engelman, *Proc. Natl. Acad. Sci. USA* **2008**, *105*, 15340 – 15345.
[14] M. An, D. Wijesinghe, O. A. Andreev, Y. K. Reshetnyak, D. M. Engelman, *Proc. Natl. Acad. Sci. USA* **2010**, *107*, 20246 – 20250.
[15] D. B. Liu, Y. Y. Xie, H. W. Shao, X. Y. Jiang, *Angew. Chem.* **2009**, *121*, 4470 – 4472; *Angew. Chem. Int. Ed.* **2009**, *48*, 4406 – 4408.
[16] X. K. Liu, M. Jiang, *Angew. Chem.* **2006**, *118*, 3930 – 3934; *Angew. Chem. Int. Ed.* **2006**, *45*, 3846 – 3850.
[17] C. Stankovic, S. Heinemann, S. Schreiber, *Biochim. Biophys. Acta Biomembr.* **1991**, *1061*, 163 – 170.
[18] X. M. Liu, B. Yang, Y. L. Wang, J. Y. Wang, *Biochim. Biophys. Acta Biomembr.* **2005**, *1720*, 28 – 34.
[19] R. Numano, S. Szobota, A. Y. Laud, P. Gorostizaa, M. Volgrafe, B. Rouxd, D. Traunere, E. Y. Isacoff, *Proc. Natl. Acad. Sci. USA* **2009**, *106*, 6814 – 6819.
[20] G. Pouliquen, C. Tribet, *Macromolecules* **2006**, *39*, 373 – 383.
[21] S. C. Sebai, S. Cribier, A. Karimi, D. Massotte, C. Tribet, *Langmuir* **2010**, *26*, 14135 – 14141.
[22] A. Walrant, I. Correia, C. Y. Jiao, O. Lequin, E. H. Bent, N. Goasdoue, C. Lacombe, G. Chassaing, S. Sagan, I. D. Alves, *Biochim. Biophys. Acta Biomembr.* **2011**, *1808*, 382 – 393.
[23] F. Burlina, S. Sagan, G. Bolbach, G. Chassaing, *Nat. Protoc.* **2006**, *1*, 200 – 205.
[24] C. Y. Jiao, D. Delaroche, F. Burlina, I. D. Alves, G. Chassaing, S. Sagan, *J. Biol. Chem.* **2009**, *284*, 33957 – 33965.
[25] F. Vial, A. G. Oukhaled, L. Auvray, C. Tribet, *Soft Matter* **2007**, *3*, 75 – 78.
[26] L. Bacri, A. Benkhaled, P. Guegan, L. Auvray, *Langmuir* **2005**, *21*, 5842 – 5846.
[27] F. Pinaud, D. King, H. P. Moore, S. Weiss, *J. Am. Chem. Soc.* **2004**, *126*, 6115 – 6123.
[28] O. Mertins, N. P. da Silveira, A. R. Pohlmann, A. P. Schroder, C. M. Marques, *Biophys. J.* **2009**, *96*, 2719 – 2726.
[29] K. Ishii, T. Hamada, M. Hatakeyama, R. Sugimoto, T. Nagasaki, M. Takagi, *ChemBioChem* **2009**, *10*, 251 – 256.

